JACS
JOURNAL OF THE AMERICAN CHEMICAL SOCIETY
Communication
pubs.acs.org/JACS

Configurationally-Coupled Protonation of Polyproline-7

Liuqing Shi,[†] Alison E. Holliday,[‡] Neelam Khanal,[†] David H. Russell,[§] and David E. Clemmer*,[†]

[†]Department of Chemistry, Indiana University, Bloomington, Indiana 47405, United States
[‡]Department of Chemistry, Moravian College, Bethlehem, Pennsylvania 18018, United States
[§]Department of Chemistry, Texas A&M University, College Station, Texas 77843, United States

Supporting Information

ABSTRACT: Structure and dynamics regulate protein function, but much less is known about how biomolecule−solvent interactions affect the structure−function relationship. Even less is known about the thermodynamics of biomolecule−solvent interactions and how such interactions influence conformational entropy. When transferred from propanol into 40:60 propanol:water under acidic conditions, a remarkably slow protonation reaction coupled with the conversion of the polyproline-I helix (PPI, having all *cis*-configured peptide bonds) into polyproline-II (PPII, all *trans*) helix is observed in this work. Kinetics and equilibrium measurements as a function of temperature allow determination of the thermochemistry and insight into how proton transfer is regulated in this system. For the proton-transfer process, PPI^{+}_{PrOH} + $H_3O^+ \rightarrow PPII^{2+}_{PrOH/aq} + H_2O$, we determine $\Delta G = -20 \pm 19$ kJ·mol^{-1}, $\Delta H = -75 \pm 14$ kJ·mol^{-1}, and $\Delta S = -188 \pm 48$ J·mol^{-1}·K^{-1} for the overall reaction, and values of $\Delta G^{\ddagger} = 91 \pm 3$ kJ·mol^{-1}, $\Delta H^{\ddagger} = 84 \pm 9$ kJ·mol^{-1}, and $\Delta S^{\ddagger} = -23 \pm 31$ J·mol^{-1}·K^{-1} for the transition state. For a minor process, $PPI^{+}_{PrOH} \rightarrow PPII^{+}_{PrOH/aq}$ without protonation, we determine $\Delta G = -9 \pm 20$ kJ·mol^{-1}, $\Delta H = 64 \pm 14$ kJ·mol^{-1}, and $\Delta S = 247 \pm 50$ J·mol^{-1}·K^{-1}. This thermochemistry yields $\Delta G = -10 \pm 29$ kJ·mol^{-1}, $\Delta H = -139 \pm 20$ kJ·mol^{-1}, and $\Delta S = -435 \pm 70$ J·mol^{-1}·K^{-1} for $PPII^{+}_{PrOH/aq}$ + $H_3O^+ \rightarrow PPII^{2+}_{PrOH/aq} + H_2O$. The extraordinarily slow proton transfer appears to be an outcome of configurational coupling through a PPI-like transition state.

While investigating the kinetics associated with structural transitions of polyproline oligomers in different solutions, we found evidence of a remarkably slow protonation event for the polyproline-7 (Pro7) oligomer, with a half-life of ∼30 min at 300 K for incorporation of the lightest and fastest chemical moiety. Unlike other naturally occurring amino acid residues, proline lacks an N−H amide group along the peptide backbone, instead utilizing the N−C$^{\alpha}$ atoms along the backbone as a part of a pyrrolidine ring.[1,2] Thus, rather than favoring *trans*-configured peptide bonds, proline residues are free to adopt both *cis* and *trans* orientations that alter biological function,[3] i.e., *cis*/*trans* isomerization of proline is associated with a variety of biological events including ion-channel gating,[4] biomolecule folding,[5] and cell signaling.[6] Proline-rich stretches are highly abundant in the huntingtin protein,[7] some antimicrobial peptides,[8] and zinc finger proteins.[9]

Polyprolines form the well-known all-*cis*, right-, and all-*trans* left-handed helices (PPI and PPII, respectively), as shown in Scheme 1.[10] These structures are sensitive to environment.[2,11]

Scheme 1. Two Views of All-*cis* PPI with Backbone Torsion angles of $\phi = -83°$, $\psi = 158°$, and $\omega = 0°$ (top) and All-*trans* PPII with $\phi = -78°$, $\psi = 149°$,and $\omega = 180°$ (bottom) helices of Pro7[a]

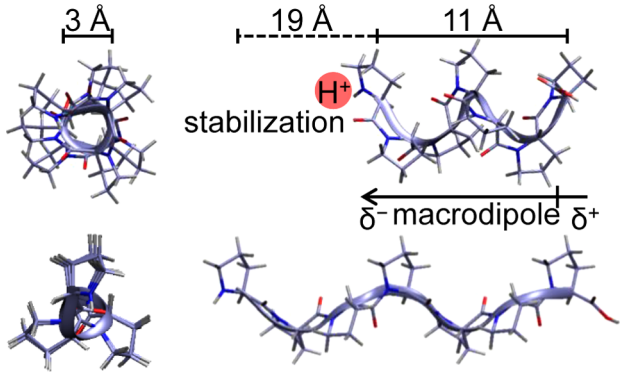

[a]An indication of length and width dimensions and charge stabilization of the macro dipole of PPI is also provided. See ref 10 for details.

The tightly folded PPI configuration excludes solvent from the peptide backbone and is favored in nonpolar solutions such as propanol. Upon immersion in water, each *cis*-configured peptide bond flips to a *trans* orientation, leading to the PPII helix that is stabilized by interactions of the exposed backbone carbonyls with the polar solvent; a configuration also found in denatured and intrinsically disordered sequences.[12] Below, we show that the PPI → PPII transition for Pro7 occurs by two mechanisms: a primary, exothermic process involving a proton transfer that proceeds through a PPI-like transition state, and a far less-efficient, entropically driven, endothermic conformational change. The intimate coupling of the protonation and configurational change leads to an unexpectedly slow rate of protonation; in fact, the slowest protonation event ever reported.

The transfer of protons in biological systems is key to a range of physiological processes from photosynthetic reaction centers, in which electron-coupled proton uptake and release are involved in multiple reaction cycles,[13] to structural changes that

Received: April 24, 2015
Published: June 26, 2015

DOI: 10.1021/jacs.5b04287
J. Am. Chem. Soc. 2015, 137, 8680−8683

give rise to macroscopic rotation of the helices that make up flagella, i.e., molecular motors.[14] In most cases it is assumed that proton transfer occurs instantaneously;[15] however, many systems appear to regulate protonation rates. For example, proton conduction in the F_0 domain of H^+-ATPase proceeds slowly, having a second-order rate constant of $k = 4 \times 10^{10}$ $M^{-1}\cdot s^{-1}$.[13] The polyproline results reported below show that even simple transitions may regulate protonation in interesting ways.

Experiments were carried out using a prototype gentle-electrospray ionization, ion mobility (IM) mass spectrometry (MS) instrument that records the mobilities of ions through a buffer gas and m/z ratios of populations of ions emanating from solution.[16] Ion mobilities (or cross sections) depend upon their shapes[17] and are sensitive to the *cis*–*trans* composition of the oligomer.[18,19] The m/z measurement determines protonation state.

Figure 1 shows that upon electrospraying 6 μM Pro7 in pure propanol (PPI@PrOH), a single peak is observed in the IM-MS distribution at m/z = 698.39, corresponding to the $[M + H]^+$ ion, having $\Omega = 188.7 \pm 1.7$ Å^2. This cross section is consistent with a previous measurement of $\Omega = 188.1$ Å^2, assigned as the PPI helix, based on detailed molecular-modeling and cross-section calculations.[19] In contrast to the α-helix,[20] the PPI helix has a macro dipole with the negative pole at the N-terminus.[21] Thus, the assigned PPI geometry has a single proton located at the N-terminal, N–H imide group,[19] as shown in Scheme 1. When Pro7 is electrosprayed from pure water (PPII@water), a single peak at m/z = 349.70, assigned to the $[M + 2H]^{2+}$ ion, is observed (Figure 1). The cross section for this ion, $\Omega = 205.0 \pm 1.5$ Å^2, is substantially greater than Ω(PPI). Molecular modeling and cross section calculations indicate that $\Omega = 205$ Å^2 corresponds to a PPII conformation that has one proton located at the N–H terminus and another on a backbone N atom associated with the seventh, C-terminal pyrrolidine ring group (See Supporting Information, SI).

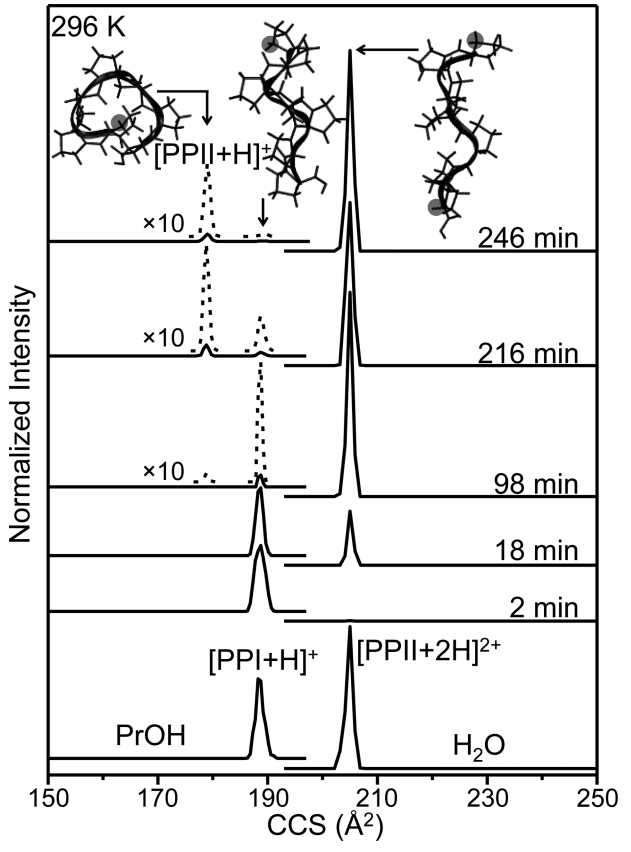

Figure 1. Cross section distributions showing the PPI → PPII transition of Pro7 in 40:59.5:0.5 1-propanol:H_2O:HOAc (v:v:v) at 296 K. Distributions obtained by electrospraying 1-propanol and H_2O are shown at the bottom. The slight offset of the $[PPI + H]^+$ and $[PPII + 2H]^{2+}$ baselines is shown to clarify that these distributions are extracted by integrating the ion intensities for ions having different m/z values. The dashed insets show blow ups of low-abundance species, and arrows are used to show the assignment of Pro7 conformations, where the dark dot indicates the charge site.

As we studied this system, it appeared that the conformation change and proton-transfer events were not instantaneous, so we investigated the kinetics. We began by incubating Pro7 in PrOH at defined temperatures for 72 h to ensure a PPI starting structure. Kinetics measurements of the proton-transfer process associated with reaction 1:

$$PPI^+_{PrOH} + H_3O^+ \rightarrow PPII^{2+}_{PrOH/aq} + H_2O \quad (1)$$

were initiated by rapid dilution of the PPI@PrOH stock solution to a final composition of 6 μM Pro7 in 60:40 water:propanol and (0.01 to 1%) acetic acid (PrOH/aq). Figure 1 shows that 2 min after dilution, ions formed from electrospraying the Pro7@PrOH/aq solution appear at the same position in the nested IM-MS distribution, indicating that PPI is initially retained. This is a remarkable result. Addition of a second proton to PPI^+@PrOH/aq to form the $PPII^{2+}$ product is extremely slow, ~10^4 times slower than the slowest reported proton-transfer process.[22]

At longer reaction times (8 min), a small peak corresponding to the proton-transfer product $PPII^{2+}$@PrOH/aq is observed; this species becomes the largest feature after ~30 min. There is no evidence for intermediates. Proton transfer appears to be coupled with the conformational change in a cooperative two-state process. Continued monitoring shows that at very long times (~100 min), a new peak corresponding to a singly protonated Pro7 is observed. These ions have $\Omega = 178.8 \pm 1.1$ Å^2, consistent with the previously reported value, $\Omega = 177.4$ Å^2, assigned to a compact, globular PPII configuration that arises from reaction 2,

$$PPI^+_{PrOH} \rightarrow PPII^+_{PrOH/aq} \quad (2)$$

when the all-*trans* PPII@aq geometry collapses upon desolvation.[19] In the absence of protonation the configurational change is less efficient. The observation that reactions 1 and 2 occur on such different time scales is an indication that these are solution-phase phenomena and not an outcome of the electrospray process.

We examine the kinetics and thermodynamics in more detail to understand how protonation is regulated. Figure 2 shows abundance profiles over time of the species in Figure 1 obtained at 278, 298, and 303 K. Analysis of these kinetics (see SI) shows that the PPI^+ precursor decays following a unimolecular pseudo-first-order rate law upon formation of the $PPII^{2+}$ product. This is the case over a 3–12 μM range of Pro7 concentrations; thus, there is no evidence that multimer formation restricts the proton-transfer rate. Studies at acetic acid concentrations (from 0.01 to 1%) show that the transition is independent of the proton concentration (i.e., zeroth order).

DOI: 10.1021/jacs.5b04287
J. Am. Chem. Soc. 2015, 137, 8680–8683

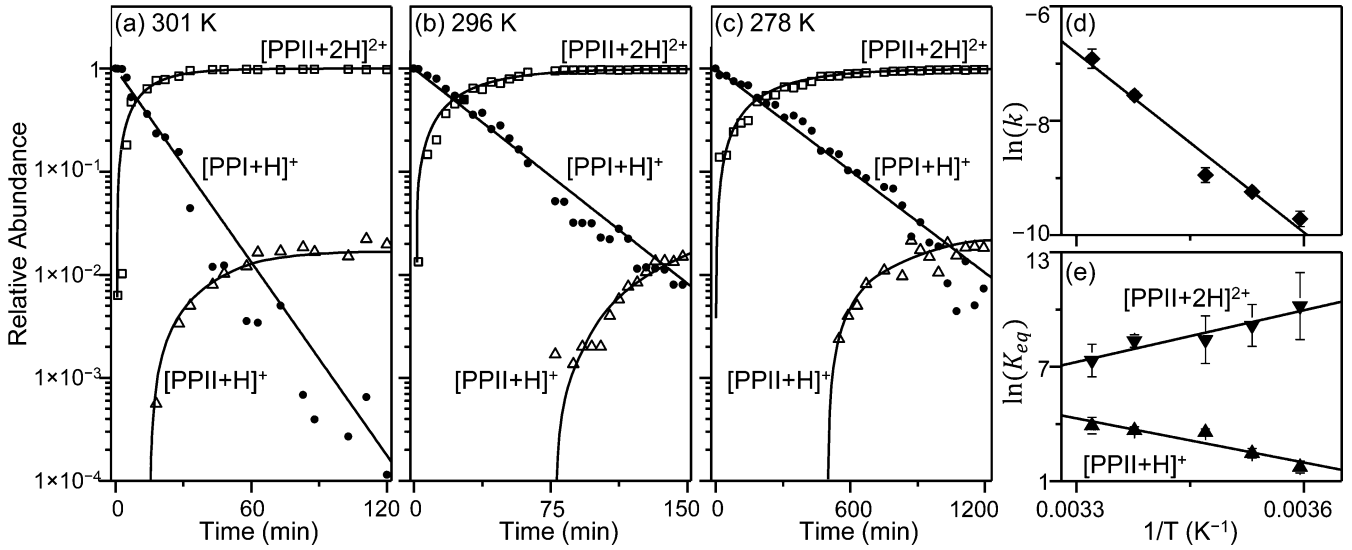

Figure 2. Relative abundance of different charge states and conformers for Pro7 as a function of transition time at (a) 301, (b) 296, and (c) 278 K. Part (d) shows an Arrhenius plot of the rate constants at five explored temperatures that is used to determine the activation barrier thermochemistry for reaction 1. Part (e) shows Van't Hoff plots of the equilibrium constants at five explored temperatures. See text and SI for details.

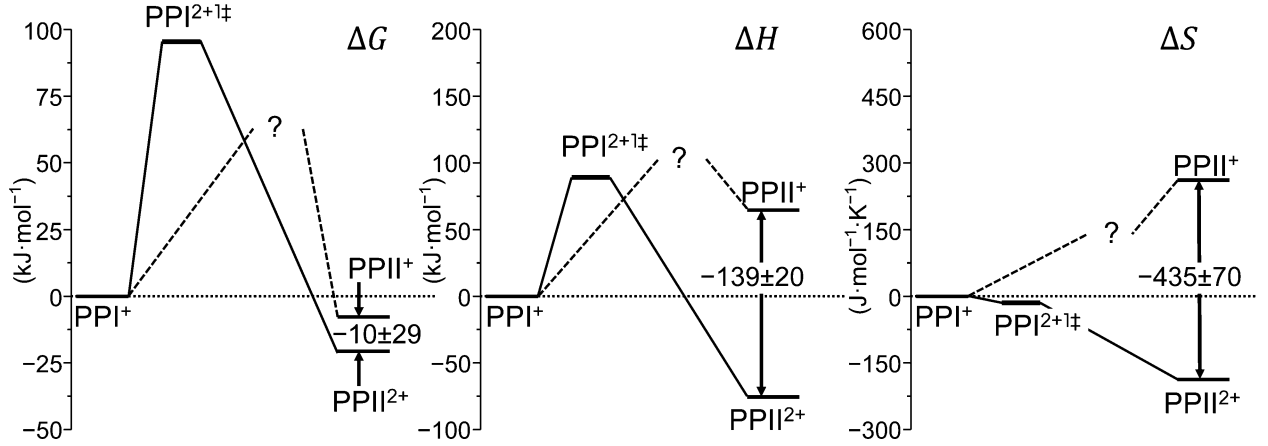

Figure 3. Experimental energy diagrams showing ΔG, ΔH, and ΔS for observed conformers of Pro7 during the PPI → PPII transition. The thermochemistry associated with the transition state for reaction 2, $PPI^+ \rightarrow PPII^+$, was not obtainable experimentally because of the induction period associated with this process and thus is shown as dashed lines and indicated by a "?". See text for details.

The less-efficient reaction 2 is also independent of the acid concentration and shows no evidence of multimer formation.

By fitting the T = 301, 296, and 278 K data sets shown in Figure 2, rate constants for reaction 1 of k = 100 ± 17, 53 ± 3, and 6.1 ± 0.8 × 10^{-5} s^{-1}, respectively, are obtained. These values (along with others measured at T = 288 and 283 K (see SI) are converted to Arrhenius plots (Figure 2) yielding transition-state thermochemistry of $\Delta G^{\ddagger}$ = 91 ± 3 and $\Delta H^{\ddagger}$ = 84 ± 9 kJ·mol^{-1}, and $\Delta S^{\ddagger}$ = −23 ± 31 J·mol^{-1}·K^{-1}. These values fall within a range of transition-state thermochemistry for stepwise *cis* → *trans* conversion measured for Pro13 in the absence of proton transfer, reported elsewhere.[18]

Temperature-dependent abundance measurements (shown in the SI) recorded when the system reaches equilibrium (i.e., long reaction times where abundances are independent of reaction time) allow us to determine the overall reaction thermochemistry. A key advantage of the IM-MS measurement is that the large dynamic range makes it possible to determine equilibrium distributions even when abundances for different species differ by many orders of magnitude. From these data, we generate the Van't Hoff plots, also shown in Figure 2, and determine: ΔG and ΔH = −20 ± 19 and −75 ± 14 kJ·mol^{-1}, respectively, and ΔS = −188 ± 48 J·mol^{-1}·K^{-1} for reaction 1; and ΔG and ΔH = −9 ± 20 and 64 ± 14 kJ·mol^{-1}, respectively, and ΔS = 247 ± 50 J·mol^{-1}·K^{-1} for reaction 2. Finally, although protonation of $[PPII + H]^+$ to form $[PPII + 2H]^{2+}$ by reaction 3

$$PPII^{+}{}_{PrOH/aq} + H_3O^+ \rightarrow PPII^{2+}{}_{PrOH/aq} + H_2O \qquad (3)$$

is not observed experimentally, its thermochemistry (ΔG and ΔH = −10 ± 29 and −139 ± 20 kJ·mol^{-1}, respectively, and ΔS = −435 ± 70 J·mol^{-1}·K^{-1}) can be derived from the values measured for reactions 1 and 2.

A summary of this thermochemistry is shown in Figure 3. The free energy plot of ΔG shows that $PPI^+ \rightarrow PPII^+$ is favorable with and without the additional protonation. The plots of ΔH and ΔS show that these processes are favored for different reasons. Reaction 2 is endothermic, driven instead by a large increase in the entropy of the system associated with the PPI → PPII configurational change. In contrast, when an

DOI: 10.1021/jacs.5b04287
J. Am. Chem. Soc. 2015, 137, 8680−8683

additional protonation accompanies the conformational change, as in reaction 1, the process is exothermic, and this energy covers the cost of ordering the system, $\Delta S = -188 \pm 48$ J·mol^{-1}·K^{-1}. The overall entropic cost associated with forming the PPII^{2+} product is much greater than what is required to reach the transition state for reaction 1, where $\Delta S^{\ddagger} = -23 \pm 31$ J·mol^{-1}·K^{-1}. This provides the clue that the critical step in regulating proton transfer (i.e., the transition state) involves protonation of the *cis*-configured PPI^{+} helix, rather than a solvated PPII^{+} helix. The doubly protonated PPI$^{2+\ddagger}$ transition state then reconfigures to the PPII^{2+} product, which is an energetically favorable, far-more-ordered state of the system.

Additional insight about how proton-transfer is regulated comes from considering the thermochemistry for reaction 3, the protonation of PPII^{+} to form PPII^{2+}. Since the oligomer has already adopted the all-*trans* PPII configuration, one might expect additional protonation to be more straightforward than protonation of PPI^{+}. The derived thermochemistry shows that protonation of PPII^{+} reaction 3 to form PPII^{2+} is highly exothermic ($\Delta H = -139 \pm 20$ kJ·mol^{-1}), and our thermochemistry suggests a favorable free energy ($\Delta G = -10 \pm 29$ kJ·mol^{-1}). But, the drastic differences in appearance times for the PPII^{2+} and PPII^{+} (Figure 3) lead us to note that there is no direct evidence for reaction 3 experimentally. Presumably this is because of the enormous entropic cost associated with the second protonation, $\Delta S = -435 \pm 70$ J·mol^{-1}·K^{-1}. While the dearth of direct evidence for reaction 3 does not rule out the direct interconversion of PPII^{+}↔PPII^{2+}, the differences in entropy suggest that equilibrium may involve a more complex process, such as PPI^{+} ↔ PPII^{+} ↔ PPI^{+} ↔ PPI$^{2+\ddagger}$ ↔ PPII^{2+}. In this way, the entropy of the system also regulates proton transfer.

With an understanding of the critical importance of entropy in regulating this proton transfer, we cannot resist speculating about the nature of the PPI-like transition state that regulates such a slow second protonation event. One might consider two extremes: Does the second proton in this system add directly to the C-terminal portion of the PPI-like peptide, or might the protonation event proceed from approach of H_3O^{+} from the N-terminal side? The latter is especially intriguing. In such a case, Coulombic interactions through the solvent as the second proton approaches could force the existing helix-stabilizing hydronium into the pore of the PPI helix. Examination of the PPI-helix pore (Scheme I) shows that the pore cavity is large enough to accommodate an interior hydronium ion (having a diameter of ∼3−4 Å) and the channel appears to be hydrophilic. Thus, as the second hydronium approaches, the initial hydronium may effectively extrude a water wire as it is forced into the helical pore. Such a mechanism may provide insight into how proton transfer occurs in larger systems.

■ ASSOCIATED CONTENT

Supporting Information

Experimental procedures, Tables S1 and S2, and Figures S1−S5. The Supporting Information is available free of charge on the ACS Publications website at DOI: 10.1021/jacs.5b04287.

■ AUTHOR INFORMATION

Corresponding Author

*clemmer@indiana.edu

Notes

The authors declare no competing financial interest.

■ ACKNOWLEDGMENTS

This work is supported in part by a grant from the NIH (R01 GM103725). We thank David Smiley of the DiMarchi Laboratory at Indiana University for assistance with the peptide synthesis.

■ REFERENCES

(1) (a) *Poly-α-amino Acids*; Fasman, G. D., Ed.; M. Dekker; New York, 1967. (b) Fischer, S.; Dunbrack, R. L., Jr.; Karplus, M. *J. Am. Chem. Soc.* **1994**, *116*, 11931−11937.

(2) Schimmel, P. R.; Flory, P. J. *Proc. Natl. Acad. Sci. U. S. A.* **1967**, *58*, 52−59.

(3) Jabs, A.; Weiss, M. S.; Hilgenfeld, R. *J. Mol. Biol.* **1999**, *286*, 291−304.

(4) Lummis, S. C. R.; Beene, D. L.; Lee, L. W.; Lester, H. A.; Broadhurst, R. W.; Dougherty, D. A. *Nature* **2005**, *438*, 248−252.

(5) Baldwin, R. L. *Annu. Rev. Biophys.* **2008**, *37*, 1−21.

(6) Sarkar, P.; Reichman, C.; Saleh, T.; Birge, R. B.; Kalodimos, C. G. *Mol. Cell* **2007**, *25*, 413−426.

(7) (a) Crick, S. L.; Ruff, K. M.; Garai, K.; Frieden, C.; Pappu, R. V. *Proc. Natl. Acad. Sci. U. S. A.* **2013**, *110*, 20075−20080. (b) Caron, N. S.; Desmond, C. R.; Xia, J.; Truant, R. *Proc. Natl. Acad. Sci. U. S. A.* **2013**, *110*, 14610−14615.

(8) Li, W.; Tailhades, J.; O'Brien-Simpson, N. M.; Separovic, F.; Otvos, L., Jr.; Hossain, M. A.; Wade, J. D. *Amino Acids* **2014**, *46*, 2287−2294.

(9) Morgan, A. A.; Rubenstein, E. *PLoS One* **2013**, *8*, e53785.

(10) IUPAC-IUB. *Biochemistry* **1970**, *9*, 3471−3479.

(11) (a) Traub, W.; Shmueli, U. *Nature* **1963**, *198*, 1165−1166. (b) Swenson, C. A.; Formanek, R. *J. Phys. Chem.* **1967**, *71*, 4073−4077. (c) Forsythe, K. H.; Hopfinger, A. J. *Macromolecules* **1973**, *6*, 423−437.

(12) (a) Adzhubei, A. A.; Sternberg, M. J. E.; Makarov, A. A. *J. Mol. Biol.* **2013**, *425*, 2100−2132. (b) Rath, A.; Davidson, A. R.; Deber, C. M. *Biopolymers* **2005**, *80*, 179−185. (c) Shi, Z.; Chen, K.; Liu, Z.; Kallenbach, N. R. *Chem. Rev.* **2006**, *106*, 1877−1897. (d) Schweitzer-Stenner, R. *Mol. BioSyst.* **2012**, *8*, 122−133.

(13) Wraight, C. A. *Biochim. Biophys. Acta, Bioenerg.* **2006**, *1757*, 886−912.

(14) Decoursy, T. E. *Physiol. Rev.* **2003**, *83*, 475−579.

(15) Marx, D. *ChemPhysChem* **2006**, *7*, 1848−1870.

(16) Hoaglund, C. S.; Valentine, S. J.; Sporleder, C. R.; Reilly, J. P.; Clemmer, D. E. *Anal. Chem.* **1998**, *70*, 2236−2242.

(17) (a) Wyttenbach, T.; Pierson, N. A.; Clemmer, D. E.; Bowers, M. T. *Annu. Rev. Phys. Chem.* **2014**, *65*, 175−196. (b) Clemmer, D. E.; Jarrold, M. F. *J. Mass Spectrom.* **1997**, *32*, 577−592.

(18) Shi, L.; Holliday, A. E.; Shi, H.; Zhu, F.; Ewing, M. A.; Russell, D. H.; Clemmer, D. E. *J. Am. Chem. Soc.* **2014**, *136*, 12702−12711.

(19) Counterman, A. E.; Clemmer, D. E. *J. Phys. Chem. B* **2004**, *108*, 4885−4898.

(20) Srebalus-Barnes, C. A.; Clemmer, D. E. *J. Phys. Chem. A* **2003**, *107*, 10566−10579.

(21) Kuemin, M.; Schweizer, S.; Ochsenfeld, C.; Wennemers, H. *J. Am. Chem. Soc.* **2009**, *131*, 15474−15482.

(22) Ritchie, C. D.; Lu, S. *J. Am. Chem. Soc.* **1989**, *111*, 8543−8544.

DOI: 10.1021/jacs.5b04287
J. Am. Chem. Soc. 2015, 137, 8680−8683